Ceramics International 42 (2016) 15224–15234

Contents lists available at ScienceDirect

Ceramics International

journal homepage: www.elsevier.com/locate/ceramint

Photosensitization of Fe_3O_4/ZnO by AgBr and Ag_3PO_4 to fabricate novel magnetically recoverable nanocomposites with significantly enhanced photocatalytic activity under visible-light irradiation

Maryam Shekofteh-Gohari, Aziz Habibi-Yangjeh *

Department of Chemistry, Faculty of Science, University of Mohaghegh Ardabili, P.O. Box 179, Ardabil, Iran

ARTICLE INFO

Article history:
Received 23 April 2016
Received in revised form
23 June 2016
Accepted 23 June 2016
Available online 24 June 2016

Keywords:
Fe_3O_4/ZnO/AgBr/Ag_3PO_4
Magnetic photocatalyst
n-n heterojunction
Visible-light-driven

ABSTRACT

In this paper, novel quaternary Fe_3O_4/ZnO/AgBr/Ag_3PO_4 nanocomposites with different weight percents of Ag_3PO_4 were successfully prepared through refluxing method at 96 °C. The as-prepared products were characterized with XRD, EDX, SEM, TEM, UV-vis DRS, FT-IR, PL, and VSM techniques to determine their phase structure, purity, morphology, spectroscopic, and magnetic properties. Photocatalytic degradation of rhodamine B under visible-light irradiation indicated that the nanocomposite with 20% of Ag_3PO_4 has the best activity. Photocatalytic activity of this nanocomposite is nearly 68, 5.0, and 3.4-folds greater than those of the Fe_3O_4/ZnO, Fe_3O_4/ZnO/AgBr, and Fe_3O_4/ZnO/Ag_3PO_4 samples in degradation of rhodamine B, whereas 17, 6.7, and 2.8-folds greater in degradation of methylene blue, respectively. The activity enhancement was mainly ascribed to the enhanced visible-light absorption ability and formation of tandem n-n heterojunctions between counterparts of the nanocomposites, which facilitate the generation and separation of charge carriers. An additional advantage of these photocatalysts is magnetic recoverability using external magnetic field. In addition, using different scavengers, superoxide ion radicals were identified as the main oxidative species in the degradation reaction of rhodamine B. Finally, photocatalytic stability of the nanocomposite was evaluated for six cycles.

1. Introduction

Environmental pollution due to the great industrial and population growth is one of the biggest challenges facing human being worldwide [1]. A promising technology to tackle this challenge is semiconductor-based photocatalytic processes using the solar energy [2]. Moreover, this technology is a promising method for conversion of solar energy, mimicking the natural photosynthesis process. Nowadays, heterogeneous photocatalytic processes have found widespread applications in different disciplines such as degradation of organic pollutants, conversion of carbon dioxide to different fuels, production of hydrogen gas by splitting of water, and disinfection of various microorganisms [3–5]. In these processes, photocatalytic reactions are started by photoinduced generation of electron-hole pairs followed by migration of these charge carriers to surface of the photocatalysts and finally surface oxidation and reduction reactions [6]. Zinc oxide is one of the most widely used photocatalyst, because of its low price and nontoxic nature. However, being as a wide band gap semiconductor, zinc oxide has poor visible-light harvesting ability. Moreover, recombination of photogenerated charge carries in this semiconductor is considerably high [7]. Visible-light absorption ability and separation of the photoinduced electron-hole pairs in photocatalysts have key roles in achieving more photocatalytic activity [8]. As a result, zinc oxide does not have remarkable photocatalytic activity under visible-light irradiation [7]. For these reasons, great efforts have been devoted to increase ability of ZnO for visible-light absorption and retard recombination of electron-hole pairs [8]. Up to now, different strategies such as metal and cation doping and combination with narrow band gap semiconductors have been proposed to enhance photocatalytic activity of ZnO under visible-light irradiation [9–11]. Among these strategies, the combination with narrow band gap semiconductors is an effective approach to improve photocatalytic activity of this wide band gap semiconductor [11–14]. The key characteristic of this strategy is formation of heterojunction between wide and narrow band gap semiconductors with matching band energies. In recent years, it was found that internal electric-field-assisted transportation of the charge carriers from one semiconductor to the other one in p-n or n-n heterojunctions of semiconductors is favorable route for enhanced separation of charge carriers in photocatalysts

* Corresponding author.
E-mail address: ahabibi@uma.ac.ir (A. Habibi-Yangjeh).

http://dx.doi.org/10.1016/j.ceramint.2016.06.158
0272-8842/

[15–19]. More importantly, we showed that by combination of three n-type semiconductors, tandem n-n heterojunctions are formed, exhibiting highly enhanced photocatalytic activities [20–22]. Zinc oxide, silver bromide, and silver phosphate are n-type semiconductors. Theoretically, by combining these semiconductors with each other, tandem n-n heterojunctions could be formed between ZnO and AgBr in one side and ZnO with Ag_3PO_4 in the other side, resulting in enhanced photocatalytic activity. The literature survey showed that there is not any report about preparation and photocatalytic activity of ZnO/AgBr/Ag_3PO_4 nanocomposites.

On the other hand, separation of photocatalysts from the treated systems involves difficulties, restricting their large-scale applications. The existence of photocatalysts in the treated water poses risk to human health. Although filtration, centrifuge, and immobilization of photocatalysts provide solutions for this drawback, these additional steps greatly increase cost of the process [23]. Magnetic photocatalysts use the idea of using external magnetic force, as a long-range attraction for separation of photocatalysts from the treated water. These photocatalysts provide a convenient approach for separation of photocatalysts from a large amount of wastewater within a short time [24–28].

In these regards, we demonstrate the fabrication of quaternary Fe_3O_4/ZnO/AgBr/Ag_3PO_4 nanocomposites with different weight percents of Ag_3PO_4, as novel magnetically separable visible-light-driven photocatalysts, using a simple refluxing method at 96 °C. The as-prepared samples were characterized for the phase structure, purity, morphology, spectroscopic, and as well as magnetic properties using X-ray diffraction (XRD), energy dispersive analysis of X-rays (EDX), scanning electron microscopy (SEM), transmission electron microscopy (TEM), Fourier transform-infrared spectroscopy (FT-IR), UV-vis diffuse reflectance spectroscopy (UV-vis DRS), photoluminescence spectroscopy (PL), and vibrating sample magnetometry (VSM) techniques. Photocatalytic activity of the Fe_3O_4/ZnO/AgBr/Ag_3PO_4 (20%) nanocomposite showed highly enhanced activity relative to the Fe_3O_4/ZnO, Fe_3O_4/ZnO/AgBr, and Fe_3O_4/ZnO/Ag_3PO_4 nanocomposites in degradations of rhodamine B (RhB), methylene blue (MB), and fuschine under visible-light irradiation, which indicates potential of the quaternary nanocomposites in sewage purification applications. In addition, these photocatalysts can be recycled conveniently by external magnetic field.

2. Experimental

2.1. Materials

Zinc nitrate ($Zn(NO_3)_2 \cdot 4H_2O$), ferric chloride ($FeCl_3 \cdot 6H_2O$), ferrous chloride ($FeCl_2 \cdot 4H_2O$), silver nitrate ($AgNO_3$), sodium bromide (NaBr), sodium hydroxide, and sodium phosphate ($Na_2HPO_4 \cdot 2H_2O$) were obtained from Loba Chemie and Rankem and used as received. Hydrochloride acid, RhB, fuschine, MB, 2-propanol, ammonium oxalate, benzoquinone, and absolute ethanol were supplied from Merck company and employed without further purification. Deionized water was used for the experiments.

2.2. Instruments

The XRD patterns were recorded by a Philips Xpert X-ray diffractometer with Cu Ka radiation (k=0.15406 nm), employing scanning rate of 0.04°/s in the 2θ range from 10° to 80°. Surface morphology and distribution of particles were studied by LEO 1430VP SEM, using an accelerating voltage of 15 kV. The purity and elemental analysis of the products were obtained by EDX on the same SEM instrument. For SEM and EDX experiments, samples mounted on an aluminum support using a double adhesive tape coated with a thin layer of gold. The TEM investigations were performed by a Zeiss-EM10C instrument with an acceleration voltage of 80 kV. The DRS spectra were recorded by a Scinco 4100 apparatus. The FT-IR spectra were obtained by a Perkin Elmer Spectrum RX I apparatus. The PL spectra of the samples were studied using a Perkin Elmer (LS 55) fluorescence spectrophotometer with an excitation wavelength of 300 nm. The conditions were fixed in order to compare the PL intensities. UV–Vis spectra for the degradation reactions were studied using a Cecile 9000 spectrophotometer. Magnetic properties of the samples were obtained using an alternating gradient force magnetometer (model AGFM, Iran). The ultrasound radiation was performed using a Bandelin ultrasound processor HD 3100 (12 mm diameter Ti horn, 75 W, 20 kHz). The pH of solutions was measured using a Metrohm digital pH meter of model 691.

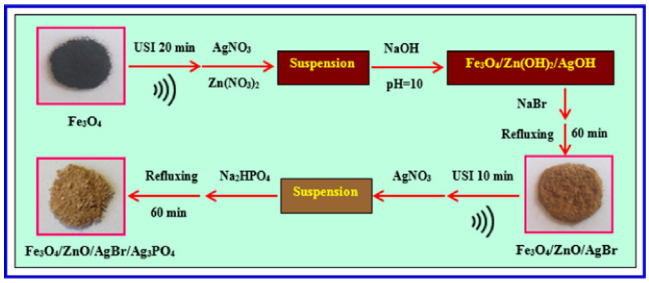

Scheme 1. Schematic illustration for the preparation procedure of the Fe_3O_4/ZnO/AgBr/Ag_3PO_4 nanocomposites.

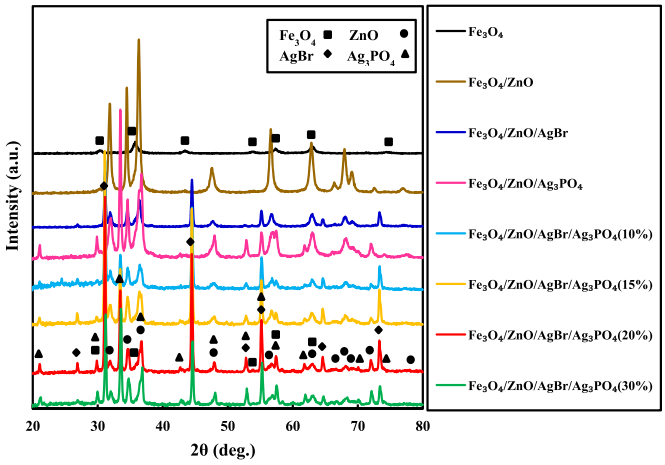

Fig. 1. XRD patterns for the Fe_3O_4, Fe_3O_4/ZnO, Fe_3O_4/ZnO/AgBr, Fe_3O_4/ZnO/Ag_3PO_4, and Fe_3O_4/ZnO/AgBr/Ag_3PO_4 samples with different weight percents of Ag_3PO_4.

2.3. Preparation of the samples

Nanoparticles of Fe_3O_4 were prepared using a chemical co-precipitation process described elsewhere [29]. The Fe_3O_4/ZnO/AgBr (1:4) nanocomposite, in which 1:4 is weight ratio of Fe_3O_4 to ZnO/AgBr, was prepared using our published procedure [30]. For preparation of the Fe_3O_4/Zn/AgBr/Ag_3PO_4 (20%) nanocomposite, where 20% is the weight percent of Ag_3PO_4, 0.4 g of the Fe_3O_4/ZnO/AgBr nanocomposite was added into 150 mL of water and dispersed by ultrasonic irradiation for 10 min. After that, silver nitrate (0.122 g) was dissolved in the suspension and mechanically stirred for 60 min. Then, an aqueous solution of sodium phosphate (0.043 g in 20 mL of water) was dropwise added to the formed suspension. Finally, the suspension was refluxed at 96 °C for